Int. J. Heat Mass Transfer. Vol. 29, No. 7, pp. 1033–1039, 1986
Printed in Great Britain

0017–9310/86 $3.00 + 0.00
Pergamon Journals Ltd.

Analysis of experiments of moisture migration caused by temperature differences in unsaturated porous medium by means of two-dimensional numerical simulation

M. PRAT

Institut de Mécanique des Fluides de Toulouse, L.A. CNRS No. 005, 2 rue Charles Camichel, 31071 Toulouse Cedex, France

(*Received* 29 *August* 1985)

Abstract—The two-dimensional aspect of the transfer resulting from the combined action of water movement due to gravity and to temperature gradients is shown; critical examination enables us to discuss the model validity and to assess the cogency of the experimental device.

1. INTRODUCTION

MANY AUTHORS have outlined the various situations, either industrial or natural, in which coupled heat and mass transfer in porous material interfere. For instance, to quote a recent publication, one can refer to Udell [1]. Among the resulting effects of coupling, the main interest centres on water movement caused by moderate temperature gradients. This movement, which could in no way be identified with thermodiffusion (a phenomenon not taken into account in the usual situations), is—in the case of the considered modelization—due to the variation of interfacial tension with temperature (as regards liquid-phase movement) and due to water vapor mass fraction (or vapor partial pressure) variations with temperature (for gas-phase transfer). Among the works dedicated to the analysis of this phenomenon, one may quote the works of Philip and De Vries [2], Cary [3], Maaledj and Le Fur [4], Cassel *et al.* [5], Bories *et al.* [6] and Crausse [7]. One can refer to Crausse *et al.* [8] for a more thorough review. To illustrate the effect of water movement due to thermal gradients, one can develop an interest in porous material drying subject to a temperature gradient as is shown in Fig. 1. Then a moisture transfer caused by temperature difference detrimental to drying is observed [9]. In the following, interest lies in the analysis of two-dimensional effects in a closed system.

2. EXPERIMENTAL LAY OUT

The porous medium considered is made of sand of almost uniform grain size diameter ($100 < d < 125$ μm). This sand is placed in a cylindrical cell 35 cm long and 5 cm in diameter. This cell is made of a 5-mm-wide Plexiglas cylinder separated from a 2-mm-wide steel cylinder by an air layer of about 1 mm, and surrounded by a 57-mm-wide insulator (Fig. 2). As will be shown later, the aim of these devices is to avoid lateral thermal leakage and consequently two-dimensional temperature distribution. The two ends of the cell are made of metal surfaces maintained at constant temperature by means of a temperature-regulated water flow. Gas-phase pressure is kept uniform and equal to atmospheric pressure by means of some vent holes. Temperatures and moisture contents of the porous material have been determined by thermocouples set along the X-axis of the cell and by cutting up the sample in 1-cm-thick slices, which are

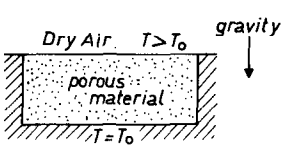

FIG. 1.

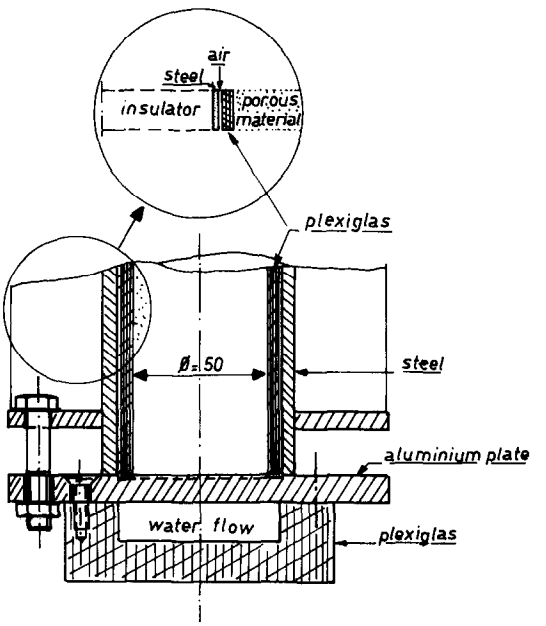

FIG. 2. Experiment cell (details).

NOMENCLATURE

A_1, B_1, A_2, B_2 coefficients
C_1, D_1, C_2, D_2 coefficients
D_ω isothermal mass diffusivity coefficient
D_T non-isothermal mass diffusivity coefficient
D_v isothermal mass diffusivity coefficient in vapor phase
D_{vT} non-isothermal mass diffusivity coefficient in vapor phase
K hydraulic conductivity
L_v latent heat of vaporization
L length of the experiment cell
l diameter or width of the experimental cell
T temperature
T_0 initial temperature
T_1 temperature of the warmer end of the cell (55°C)
t time
t_i time scale, $i = 1, \ldots, 11$
x axial coordinate
y axial coordinate
z axial coordinate.

Greek symbols
λ^* apparent thermal conductivity of the porous material
$(\rho C)^*$ volumetic heat capacity
ρ_e water density
ρ_0 density of dry material
ω moisture content [kg/kg]
ω_0 initial moisture content
ω_s moisture content scale (saturation).

separately weighed and desiccated in a dry kiln. Given uniform temperature and moisture content (ω_0, T_0) as initial conditions, the experimental process consists of analysing the moisture contents' and temperatures' space—time evolution when the thermodynamic equilibrium is broken by setting the $X = 0$ section to $T_1 > T_0$ (Fig. 3). As far as the experiments described and analysed here are concerned the temperature difference has always been 34°C with initial conditions of respectively 21°C and 11.2%, and 21°C and 6.6%. Extra details concerning these experiments can be found in Crausse's thesis [7].

3. MATHEMATICAL FORMULATION

Considering an unsaturated, nondeformable, homogeneous, isotropic porous medium and assuming that the total pressure in the gas phase is uniform and that there is no chemical reaction, and neglecting compressional work, viscous dissipation and convective terms in the energy equation and considering the gas-phase mass transport equation for the evaporating species as quasi-steady, equations describing heat and mass transfer phenomena in such media are generally the following:

$$\frac{\partial \omega}{\partial t} = \nabla \cdot [D_\omega \nabla \omega + D_T \nabla T] - \nabla \cdot \left[\frac{\rho_e}{\rho_0} K \nabla z\right] \quad (1)$$

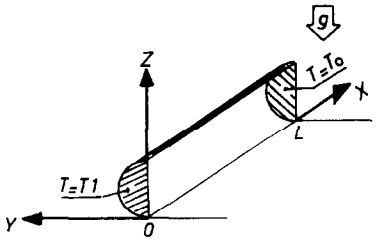

FIG. 3.

$$(\rho C)^* \frac{\partial T}{\partial t} = \nabla \cdot [(\lambda + L_v \rho_0 D_{vT}) \nabla T] + \nabla \cdot [L_v \rho_0 D_v \nabla \omega]. \quad (2)$$

Here the gas- and liquid-phase mass conservation equations have been summed up. The phase-change term is not explicitly apparent. All coefficients of equations (1) and (2) are dependent variables of moisture content and temperature and have been studied from specific experiments by Crausse [7] regarding the porous medium considered. The above model has been validated although with some reservations. As a matter of fact the validation has been obtained by comparing monodimensional numerical simulation and experimental results. Consequently neither gravity nor wall heating effects have been taken into account.

4. NUMERICAL SOLVING METHOD

The resolution of this kind of strongly non-linear equation has been the object of numerous publications. In the monodimensional case we can quote Vauclin *et al.*'s work [10] concerning finite-difference methods. Finite-difference methods have been used in two- and three-dimensional geometry. One may for instance refer to Nakamo *et al.* [11] for a three-dimensional case. For reasons of flexibility in the mesh choice and with the aim of taking into account Neuman conditions with a view to applications to other problems, we used a finite-element method. In two-dimensional geometry the domain under consideration is cut up and rectangular elements. The method is in fact a Galerkin method based on linear interpolation. The solving principle, very similar to the one described by Bacon [12] in the monodimensional case, leads us to a system using Newton's method:

$$A_1 W^{m+1} = B_1 W^m + C_1 T^{m+\theta} + D_1 \quad (3)$$

$$A_2 T^{m+1} = B_2 T^m + C_2 W^{m+\theta} + D_2. \quad (4)$$

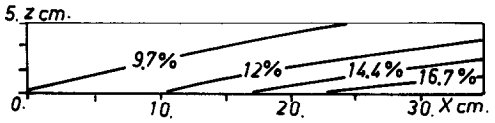

FIG. 4. Moisture content distribution (steady-state regime, $\omega_0 = 11.2\%$).

The resolution is carried out by using a direct Gauss elimination method successively for each equation. The resolution is obtained when the difference between two successive iterations is smaller than a given value. The simulation of the transfers in the vertical median plane including the X-axis (Fig. 3) is performed with a mesh of 175 square elements.

5. RESULTS AND DISCUSSION

In order to appreciate the influence of a two-dimensional effect induced by gravity and thermal interactions, three occurences have been simulated and confronted with experimental results; two occurences of permanent state regime for initial conditions $\omega_0 = 11.2\%$ and $\omega_0 = 6.6\%$; and one occurrence of transient state regime for initial conditions $\omega_0 = 11.2\%$. In order to make a comparison with experimental data, the moisture contents considered are the vertical-slice average moisture contents. Unless otherwise mentioned, as we have previously stipulated, we simulate transfer in the plane defined as the median vertical enclosing the X-axis plane.

Steady-state regime

Figure 4 gives moisture content distribution in the case of initial moisture content at 11.2%. This distribution precisely shows the two-dimensional aspect of transfers resulting from vertical movement due to gravity and horizontal movement due to thermal gradient combined action. Figure 5 demonstrates how seriously we have to take gravity into account when experimental and numerical results are being compared. In a transient state regime study we will attempt to give the reasons for differences when gravity is or is not taken into account in the simulation; that is to say how the differential action of the thermal gradients is working according to the moisture content. The effect of gravity is all the more sensitive the higher the initial moisture content. It should be noted that considering higher initial moisture contents (for instance $\omega_0 = 14.2\%$ in the case of the simulation we made), the combined effect of gravity and thermal gradients causes a saturated zone in the lower, cold end of the cell. In this case (already mentioned by Firdaouss *et al.* [13]), we face the problem of coupling a non-saturated zone with a saturated zone—a case which is not studied here. Such a case has already been investigated by Vauclin *et al.* [14]. In the 6.6% case a less sensitive gravity action can be observed.

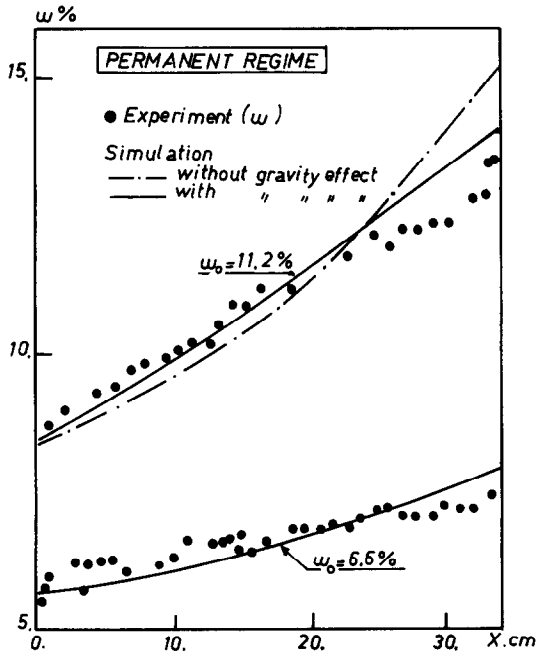

FIG. 5. Comparison between simulation and experiment (steady-state regime).

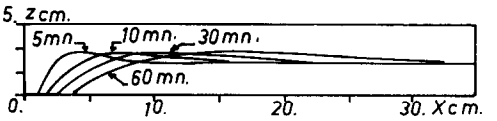

FIG. 6. 11.2% moisture content line time evolution.

Transient state regime

Simulations were performed with an initial moisture content of 11.2%. Figure 6 shows the 11.2% moisture-content-line time evolution. Figures 7 and 8 give the temperature and the moisture content distribution after 1 h. It should be mentioned that the isotherms are not strictly vertical. The difference between the upper and lower part is about 0.1°C in the warmer zone. The time isotherm evolution is slower in the higher moisture content zone; this agrees with the material thermal diffusivity considered since we are in the 0.07–0.16% moisture content zone in which the thermal diffusivity coefficient decreases according to moisture content (Fig. 9).

As regards the different processes, it is interesting to study time scales of the different phenomena under

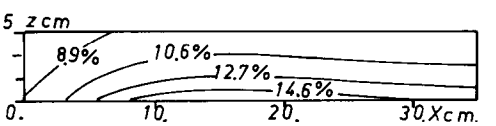

FIG. 7. Moisture content distribution ($\omega_0 = 11.2\%$).

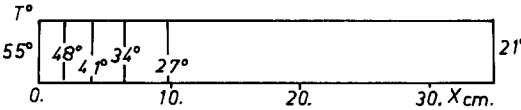

FIG. 8. Isotherms ($\omega_0 = 11.2\%$).

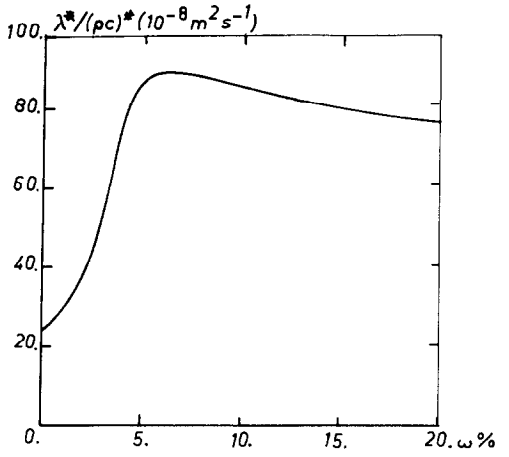

FIG. 9. Thermal diffusivity of the material.

consideration (diffusion, gravity, heat conduction, latent energy transfer). With this in mind we write:

$$\omega^* = \omega/\omega_s; \quad T^* = (T-T_0)/(T_1-T_0);$$
$$x^* = x/L; \quad z^* = z/l; \quad t^* = t/t_r. \tag{5}$$

The mass conservation equation leads to:

$$\frac{1}{t_r}\frac{\partial\omega^*}{\partial t^*} = \frac{\partial}{\partial x^*}\left(\frac{1}{t_1}\frac{\partial\omega^*}{\partial x^*} + \frac{1}{t_2}\frac{\partial T^*}{\partial x^*}\right) + \frac{\partial}{\partial z^*}\left(\frac{1}{t_4}\frac{\partial\omega^*}{\partial z^*} + \frac{1}{t_5}\frac{\partial T^*}{\partial z^*} - \frac{1}{t_3}\right) \tag{6}$$

with $t_1 = L^2/D_\omega$ being the time scale of mass diffusion due to the moisture content gradient along $0X$; $t_2 = L^2\omega_s/D_T(T_1-T_0)$ the time scale of mass diffusion due to the thermal gradient along $0X$; $t_3 = l\rho_s\omega_s/\rho_e K$ the time scale of water movement due to gravity; $t_4 = l^2/D_\omega$ the time scale of mass diffusion due to the moisture content gradient along $0Z$; and $t_5 = l^2\omega_s/D_T(T_1-T_0)$ the time scale of mass diffusion due to the thermal gradient along $0Z$. (It should be noted that the temperature scale we have to consider is in this case $T_H - T_B$, i.e. the maximum difference along the vertical between the lower part and the upper part of the cell.)

Concerning the heat transfer equation, we have:

$$\frac{1}{t_r}\frac{\partial T^*}{\partial t^*} = \frac{\partial}{\partial x^*}\left[\left(\frac{1}{t_6}+\frac{1}{t_7}\right)\frac{\partial T^*}{\partial x^*} + \frac{1}{t_8}\frac{\partial\omega^*}{\partial x^*}\right] + \frac{\partial}{\partial z^*}\left[\left(\frac{1}{t_9}+\frac{1}{t_{10}}\right)\frac{\partial T^*}{\partial z^*} + \frac{1}{t_{11}}\frac{\partial\omega^*}{\partial z^*}\right] \tag{7}$$

with $t_6 = (\rho C)^* L^2/\lambda^*$ being the time scale of heat transfer due to conduction along $0X$; $t_7 = (\rho C)^* L^2/L_v\rho_0 D_{vT}$ the time scale of latent energy transfer due to the thermal gradient along $0X$; $t_8 = (T_1-T_0)(\rho C)^* L^2/L_v\rho_0 D_v\omega_s$ the time scale of latent energy transfer due to the moisture content gradient along $0X$; $t_9 = (\rho C)^* l^2/\lambda^*$ the time scale of heat transfer due to conduction along $0Z$; $t_{10} = l^2(\rho C)^*/L_v\rho_0 D_{vT}$ the time scale of latent energy transfer due to the thermal gradient along $0Z$ (for the same reason as above, the temperature difference considered is $T_H - T_B$); and $t_{11} = l^2(T_1-T_0)(\rho C)^*/L_v\rho_0 D_v\omega_s$ the time scale of latent energy transfer due to the moisture content along $0Z$.

For the moisture content and temperature ranges and the length scales considered we obtain the following classification: concerning mass transfer along $0X$, $t_2 < t_1$; along $0Z$, $t_3 < t_4 \ll t_5$; concerning energy transfer along $0X$, $t_6 \ll t_7 < t_8$; along $0Z$, $t_9 \ll t_{11} < t_{10}$; with also $t_4 < t_1$ and $t_9 < t_6$.

The classification obtained shows that, considering the small temperature differences along $0Z$ (isotherms nearly vertical), the evolution towards equilibrium results

- along $0Z$ from a competition between mass flux due to gravity and mass flux due to moisture gradients;
- along $0X$ from a competition between mass flux due to thermal gradients and mass flux due to moisture gradients.

Concerning heat transfer, we deduce that is is practically monodimensional along X and we can therefore discard vaporization–condensation effects [15] given by the following simple equation:

$$(\rho C)^*\frac{\partial T}{\partial t} = \frac{\partial}{\partial x}\left(\lambda^*\frac{\partial T}{\partial x}\right). \tag{8}$$

These considerations allow us to understand the water redistribution process inside the material. Gravity acts very quickly compared to water movement due to thermal gradients (which, in an early experiment, were found to only concern the part near the 55°C cell end) and brings about a stratification along the vertical. Water movement due to thermal gradients alters this water redistribution in two ways: at one end by horizontal water movement (drainage of the warmer zone and imbibition of the colder zone) and at the other end by a slight change of the gravity equilibrium leading to new vertical movements. The interaction between water movement due to gravity and water movement due to thermal gradients can be shown by means of numerical simulation. In this view we take as initial conditions the isothermal stratification due to gravity at $T = 21$ C and we compare the results deriving from these new initial conditions when we take into account gravity effects and when only horizontal movement are considered. This slight modification of gravity equilibrium is due to the change in the isothermal mass diffusivity coefficient and in the hydraulics conductivity. Figures 10 and 11, which show mass flux density evolution after 1 h near the upper and lower boundaries of the cell, exemplify the modification. In the upper part the moisture content is lower and as the isothermal and non-isothermal mass diffusivity coefficients are increasing with moisture content in the moisture content range under consideration, the horizontal water movement is relatively slower in this part than in the lower part,

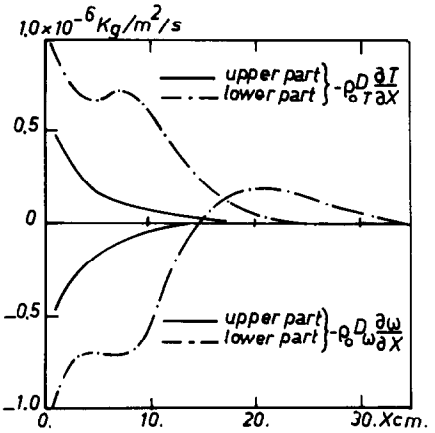

FIG. 10. Horizontal mass flux density space evolution (mass flux density due to horizontal moisture content gradients and mass flux density due to horizontal thermal gradients); $t = 60$ min.

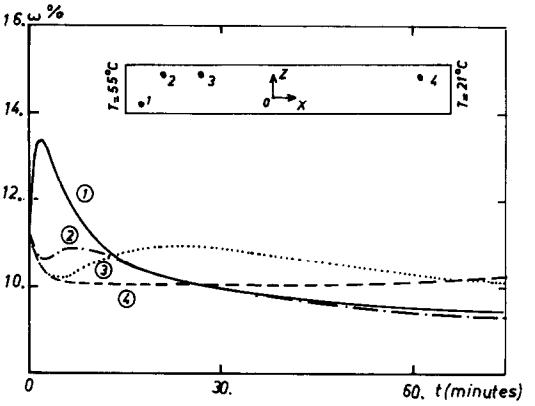

FIG. 12. Moisture content time evolution concerning four points of the cell.

hence a change in the gravity equilibrium and water redistribution. It should be noted that the gravity equilibrium is also changed by heat transfer (hydraulic conductivity and isothermal mass diffusivity coefficient change with temperature).

At the end of this precise local analysis in which the distinctly two-dimensional character acting in the described experiments has been shown, we have to examine the consequences upon the only quantities deduced from the experiments, i.e. variation of moisture content average values in vertical slices on X—these elements form the basis together with the previously performed monodimensional simulation. With this aim in view the calculation of average values in each vertical slice was made from the two-dimensional moisture content distribution at $t = 60$ min. The comparison of these average values with those previously obtained is shown in Fig. 13. This clearly demonstrates that the effect of gravity is not the underlying factor in the discrepancy between experiment and simulation.

At this stage of the analysis, this discrepancy can be

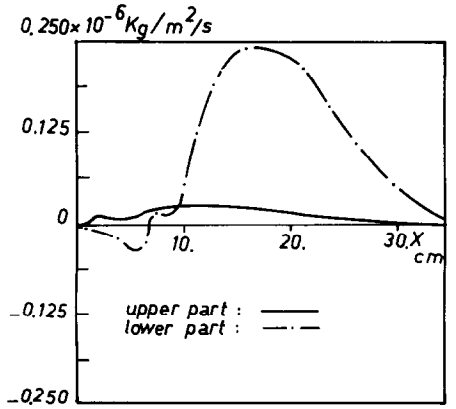

FIG. 11. Horizontal total mass flux density space evolution; $t = 60$ min.

derived from three effects. These are the following:

—one hysterisis effect since, as a whole, the colder zone is under imbibition whereas the warmer zone is under drainage. (It should be noted as is shown in Fig. 12 that the mass transfer is locally rather more complex). This effect was not taken into account in simulation. Taking this phenomena into account is likely to greatly improve the results as suggested by the anlysis made in ref. [7].

—one three-dimensional effect caused by the geometrical shape of the cell which leads to particular water accumulation zones.

—one wall heat transfer effect due to the particular structure of the cell.

The three-dimensional effect

In order to study this effect the circle obtained by cutting up transversely the cylinder was approximated, for reasons of numerical simplicity, not by means of a square—as in the previous case—but by a rhomb.

Figure 14 shows the distribution due to gravity obtained at the very same moment in these two situations under isothermal conditions. The analysis consisted on one hand of making up a new moisture content distribution along the vertical from horizontal-slice average values obtained in the rhomb case when the permanent regime is under isothermal conditions ($T = 21°C$) is reached and on the other hand of studying the effect of the horizontal thermal gradient 1 h after starting from these new initial conditions. This procedure, the validity of which has been previously substantiated in the square case, did not lead us to a significant modification of the results shown in Fig. 13. Since a three-dimensional numerical code was not being used, the results obtained until now appear to confirm definitely that gravity is not the determining factor of the discrepancy between simulation and experiment.

Wall heat transfer effect

In fact we deal with the problem of an unwanted heating of the porous medium due to differences in

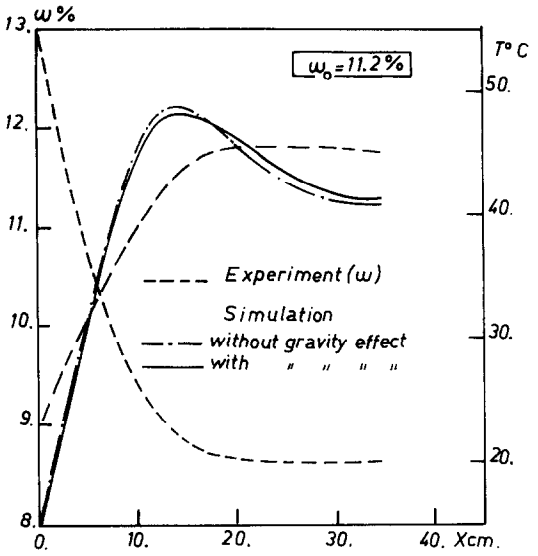

FIG. 13. Comparison between experiment and simulation (transient regime; $t = 60$ min).

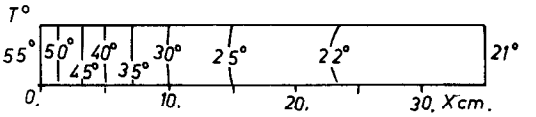

FIG. 15. Isotherms taking into account heat wall transfer effect.

conditions ($T = 21$°C). The aspect of the isotherm lines obtained in the porous medium exemplifies this wall-heating effect. The comparison between simulation and experiments (Fig. 16) shows a fairly visible sensitivity of transfer to this wall-heating effect.

Lastly we considered the case in which the gaseous phase pressure was not uniform and not equal to atmospheric pressure. (In this case equations were then similar to those considered by Moyne *et al.* [16] but written in two-dimensional geometry). If we suppose the cell to be completely closed, we observe a fairly quick return to pressure uniformity and no mass transfer due to gaseous phase pressure gradients likely to notably improve results.

thermal diffusivity coefficients of the different components of the cell walls (Fig. 2). This effect has been studied taking into account the succession of Plexiglas, steel, and insulator cylinders constituting the cell and the air layer separating Plexiglas from steel. (The mesh is no longer 175 elements of identical size but now consists of 595 elements of variable size which allows us to solve simultaneously heat transfer equations in each cylinder constituting the cell.) The boundary conditions, for the energy equation, along the horizontal walls are no longer zero-flux conditions but Dirichlet

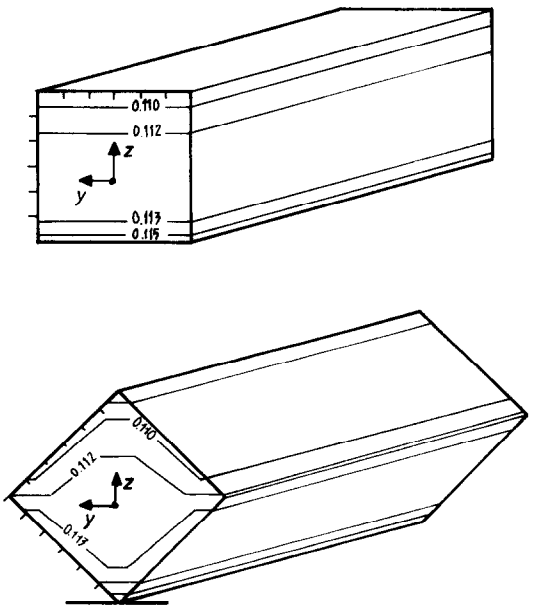

FIG. 14. Moisture content distribution line in rhomb case and in square case at the same moment.

6. CONCLUSION

The critical examination of these experiments in permanent and transient regimes by means of two-dimensional numerical simulation allowed us to appreciate the influence of the mechanisms at work and to demonstrate the peculiarities of the transfers in the experimental cell resulting from the combined action of gravity, and water movement due to thermal gradients. In the present state of our analysis, the hysteresis phenomenon in the presence of thermal gradients—which is the present object of specific studies—is the last effect whose influence is to be understood. Presently this analysis gives all the elements allowing us to make experiments in the best conditions.

In particular the wall-heating effect influence clearly

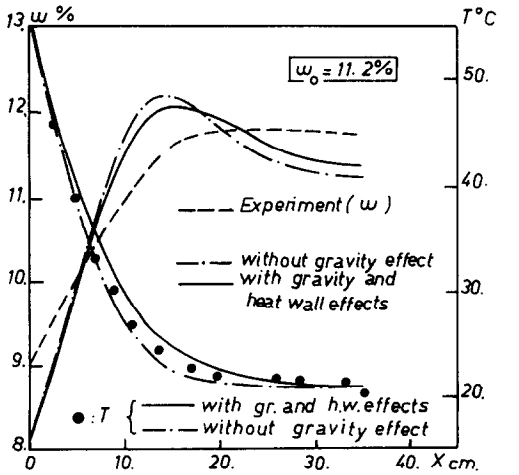

FIG. 16. Comparison between experiment and simulation (transient regime; $t = 60$ min).

exemplifies the precautions to be taken in the working out of such experiments when thermal gradients take place.

Acknowledgements—The author is very thankful to S. Bories, P. Crausse and G. Bacon for discussions and comments during the course of investigation.

REFERENCES

1. K. S. Udell, Heat transfer in porous media considering phase change and capillarity—the heat pipe effect, *Int. J. Heat Mass Transfer* **28,** 485–495 (1985).
2. J. Philip and D. A. De Vries, Moisture movement in porous materials under temperature gradients, *Trans. Am. geophys. Un.* **38,** 222–232 (1957).
3. J. W. Cary, Soil moisture transport due to thermal gradients: practical aspects, *Soil Sci. Soc. Amer. Pr.* **30,** 428–433 (1966).
4. M. Maaledj et B. Le Fur, Theories et expériences sur la thermomigration de l'eau dans les milieux poreux, *Proc. 4th. Int. Heat Transfer Conf.*, Versailles, France (1970).
5. D. K. Cassel, D. R. Nielsen and J. W. Biggar, Soil water movement in response to imposed temperature gradients, *Soil Sci. Soc. Am. Proc.* **32,** 183–189 (1969).
6. S. Bories et P. Crausse *et al.*, Thermomigration en milieu poreux—évolution de la zone sèche en système fermé, *C. R. hebd. Séanc. Acad. Sci., Paris* **280B,** 29–31 (1975).
7. P. Crausse, Etude fondamentale des transferts couplés de chaleur et d'humidité en milieu poreux non saturé. Thèse doctorat d'etat, I.N.P. Toulouse (1983).
8. P. Crausse, G. Bacon et S. Bories, Etude fondamentale des transferts couplés chaleur–masse en milieu poreux, *Int. J. Heat Mass Transfer* **24,** 991–1004 (1981).
9. S. Bories, G. Bacon and M. Recan, Experimental and numerical study of coupled heat and mass transfer in porous materials, *Proc. 4th Int. Drying Symposium*, pp. 159–164, Kyoto, Japan (1984).
10. M. Vauclin, R. Haverkampf et G. Vachaud, *Résolution numérique d'une équation de diffusion non linéaire. Application à l'infiltration de l'eau dans les sols non saturés.* Presses Universitaires de Grenoble (1979).
11. Y. Nakamo, T. Cho and D. Hillel, Effect of transient, partial area shading on evaporation from a bare soil, *Soil Sci.* **135,** 282–295 (1983).
12. G. Bacon, Simulation numérique des transferts de chaleur et de masse dans un milieu poreux non saturé, Colloque sur les transferts de chaleur et de masse en milieu poreux non saturé, Lausanne (1982).
13. M. Firdaouss et M. Mabsate, simulation numérique de la thermomigration bidimensionnelle. Influence du potentiel gravitaire, *Communication Congrés Euromech 194*, Nancy, France (1985).
14. M. Vauclin, D. Khanji et B. Vachaud, Etude et expérimentale et numérique du drainage et de la recharge des nappes à surface libre avec prise en compte de la zone non saturée, *J. Méc.* **15,** 307–340 (1976).
15. S. Bories, G. Bacon et D. Monferran, Influence de la teneur en eau et de la température sur la conductivité thermique des milieux poreux non saturés, *Septième Symposium International de l'A.I.R.H.* (1980).
16. C. Moyne, and A. Degiovanni, Importance of gas phase momentum equation in drying above the boiling point of water, *Proc. 4th Int. Drying Symposium*, pp. 119–126, Kyoto, Japan (1984).

ANALYSE PAR SIMULATION NUMERIQUE BIDIMENSIONNELLE D'EXPERIENCES DE THERMOMIGRATION EN MILIEU POREUX

Résumé—L'aspect bidimensionnel des transferts qui résulte de l'action combinée de la gravité et des gradients thermiques est mis en évidence. Une analyse critique permet ensuite d'examiner la validité du modèle et de juger du bien-fondé du dispositif expérimental.

UNTERSUCHUNG DER THERMISCH BEDINGTEN FEUCHTIGKEITSWANDERUNG IN UNGESÄTTIGTEN SCHÜTTUNGEN MITTELS ZWEIDIMENSIONALER NUMERISCHER SIMULATION

Zusammenfassung—Es zeigt sich, daß die Feuchtigkeitsbewegung infolge der kombinierten Einflüsse von Schwerkraft und Temperaturgradienten zweidimensional ist. Ein kritischer Vergleich erlaubt es, die Gültigkeit des Modells und die Qualität der vorhandenen Versuchseinrichtung zu beurteilen.

АНАЛИЗ ЭКСПЕРИМЕНТОВ ПО МИГРАЦИИ ВЛАГИ, ВЫЗВАННОЙ РАЗНОСТЬЮ ТЕМПЕРАТУР В НЕНАСЫЩЕННОЙ ПОРИСТОЙ СРЕДЕ, С ПОМОЩЬЮ ДВУМЕРНОГО ЧИСЛЕННОГО МОДЕЛИРОВАНИЯ

Аннотация—Исследуется двумерное движение воды, обусловленное гравитацией и температурными градиентами. Обсуждается принцип применимости модели, оцениваются достоинства экспериментального устройства.